Nakata et al., http://www.jcb.org/cgi/content/full/jcb.201104034/DC1

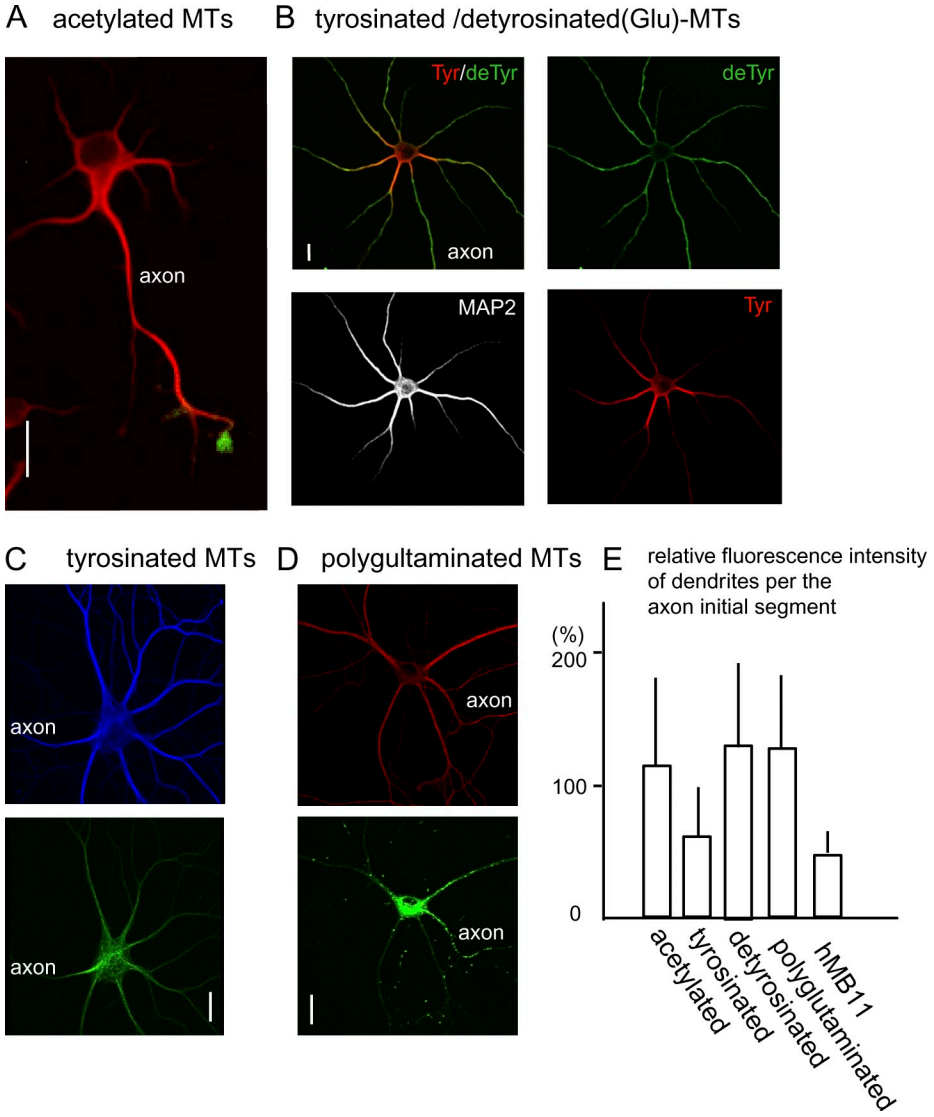

Figure S1. **Posttranslational modification of tubulins.** (A) Labeling for tubulin acetylation (red) and truncated KIF5 (green) at the tips of axons in stage 3 neurons. (B) Labeling for tubulin detyrosination (green), tubulin tyrosination (red), and MAP2 (white) in a stage 5 neuron. Detyrosinated (Glu) tubulin uniformly localized in somatodendrites and axon initial segments, whereas tyrosinated tubulin localized mainly in proximal dendrites and the axon initial segment. (C) Double labeling of tubulin tyrosination (blue) and rigor kinesin (green), which preferentially binds axonal MTs (Nakata and Hirokawa, 2003). (D) Double labeling of polyglutaminated MTs (red) and post-Golgi axonal VSV-G transport (green). These posttranslational modifications of MTs were not so specific for axons (or dendrites). Bars, 10 µm. (E) Quantification of the relative fluorescence intensity of posttranslational modifications of dendrites in the initial segments of axons. For acetylated, detyrosinated, and polyglutaminated MTs and hMB11 staining as a control, the most intensely stained dendrites were compared with the axon initial segments in the same neuron, and the fluorescence ratio was presented as a percentage. For tyrosinated MTs, the least intense stained proximal dendrites were compared with the axon initial segment in the same neuron, as the modification is assumed to be inhibitory. Error bars indicate standard deviation (n = 33–52).

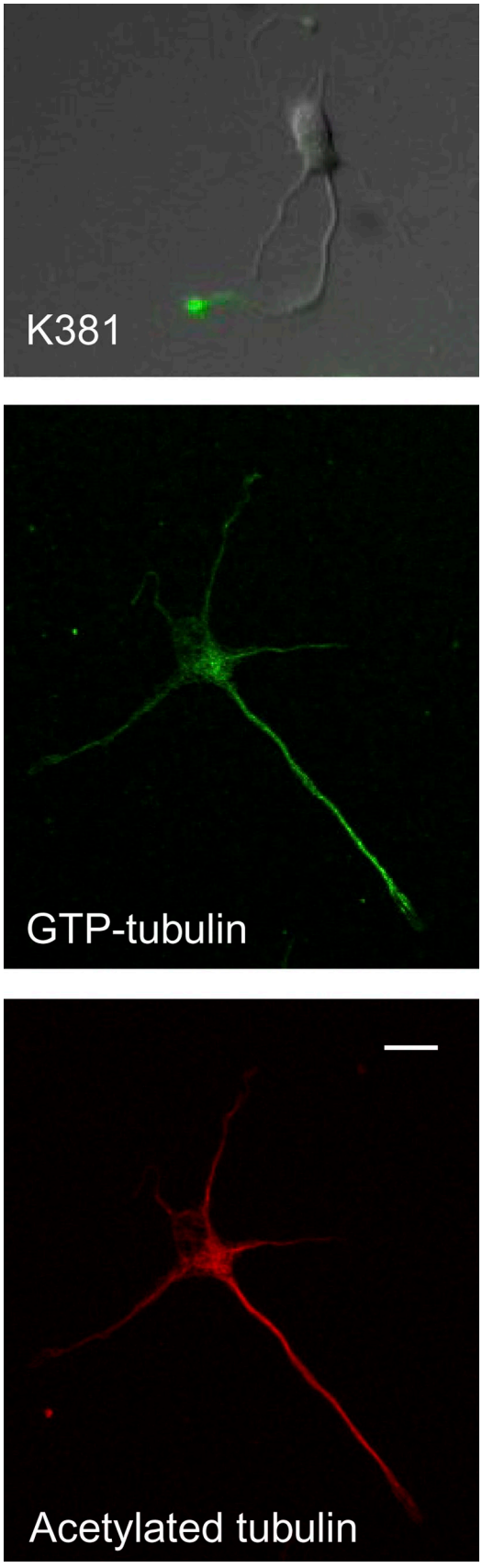

Figure S2. **Effect of HDAC6 inhibitor on axonal specification.** Truncated KIF5C accumulated to the tip of one neurite of a stage 2 neuron, even in the presence of 5 μM trichostatin A (top). The localization of GTP-tubulin (middle) as well as acetylated tubulin (bottom) was not affected significantly. Bar, 10 μm.

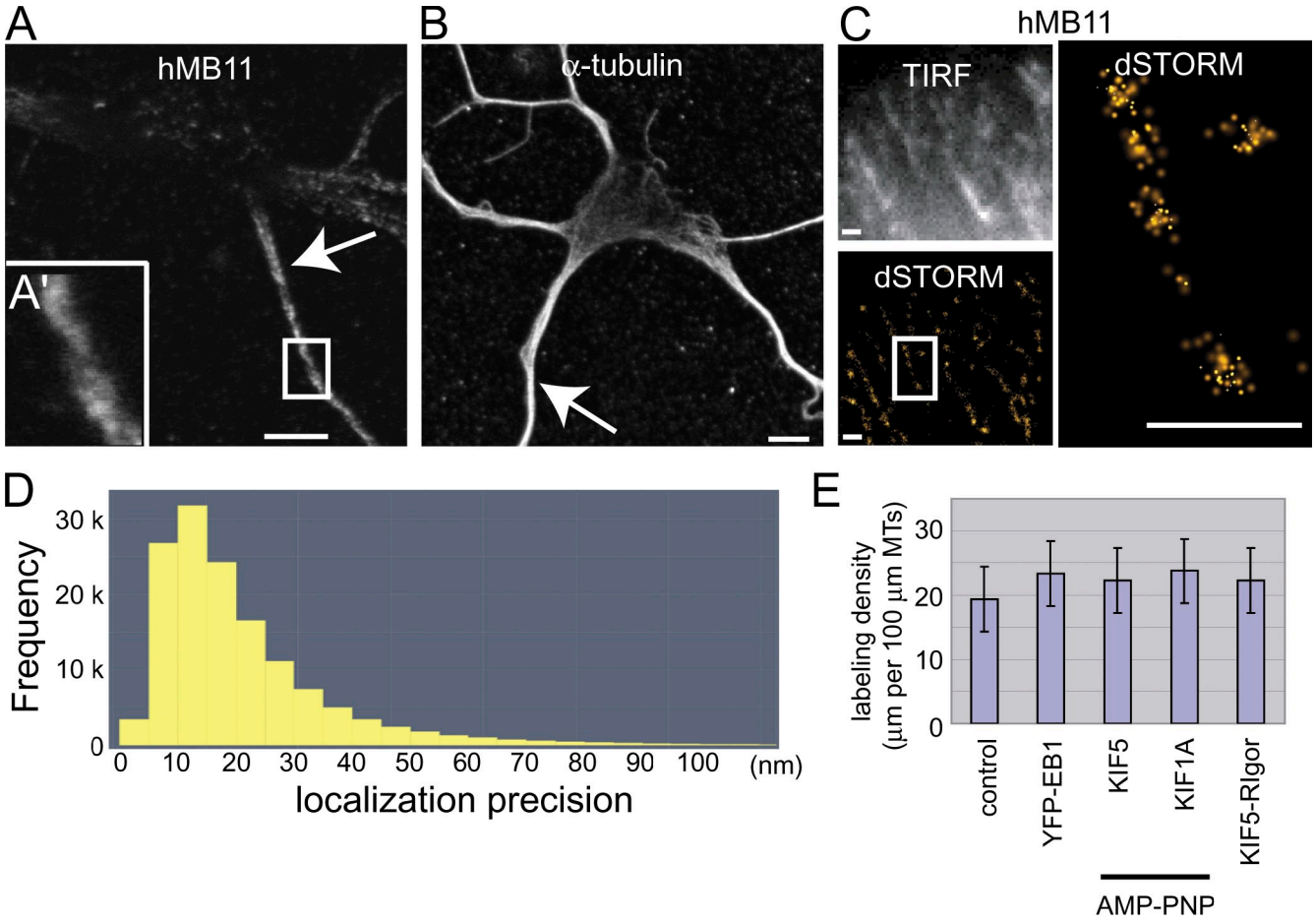

Figure S3. **Superresolution microscopy of GTP tubulin.** (A, A′, and B) Confocal microscopy images of hMB11 staining (A and A′) and anti–α-tubulin antibody staining (B) together with ATTO565 secondary antibody labeling. A′ shows a magnification of the boxed area in A. Note that hMB11 staining was more abundant in axons (arrows), whereas α-tubulin staining was not polarized. Bars, 25 μm. (C) Comparison of conventional microscopy (TIRF) and superresolution microscopy (dSTORM) using blinking of ATTO565 (van de Linde et al., 2009). The top shows a magnified view of the boxed area. Note that the spatial resolution is higher in dSTORM than in TIRF. Bar, 500 nm. (D) An example of a histogram showing the localization precision of ATTO565 fluorophores. (E) Labeling density of hMB11 staining in control, YFP-EB1–transfected, Dronpa-K381–transfected (KIF5), Dronpa-C381–transfected (KIF1A), and Dronpa-K381 rigor–transfected (KIF5-Rigor) cells. KIF5- or KIF1A-transfected cells were observed in the presence of 5 mM AMP-PNP. Labeling density of hMB11 per 100 μm MT was measured. 100 MTs from 10 independent samples were measured and averaged. The graph presents means ± SD. The data are statistically not different (*t* test).

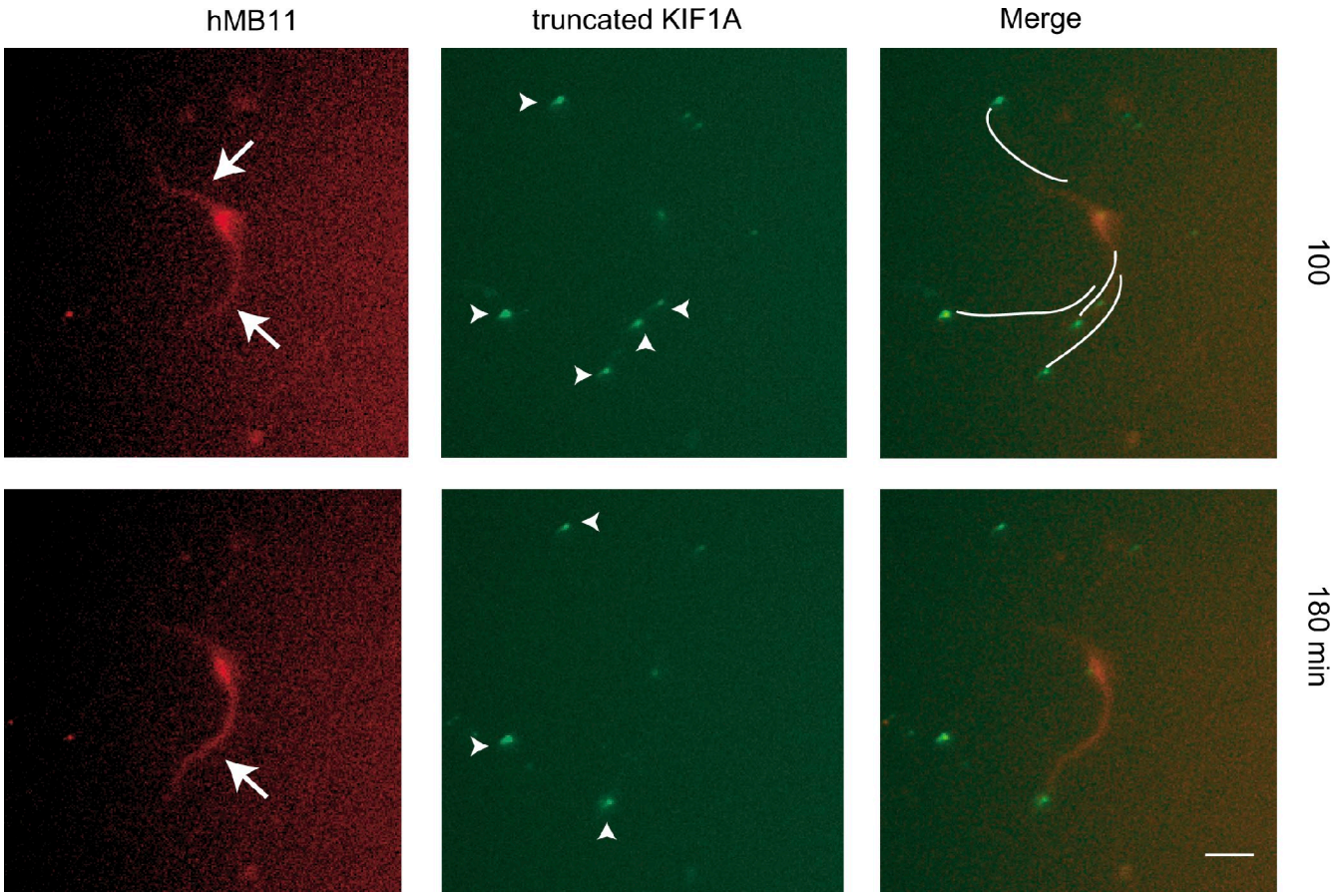

Figure S4. **Dynamics of truncated KIF1A and hMB11-mCherry in stage 2 neurons.** Truncated KIF1A localized at multiple tips (arrowheads), whereas hMB11 localized in only 1–2 neurites (arrows) at a time. Lines in merged images show the contour of the neuron. Bar, 10 µm.

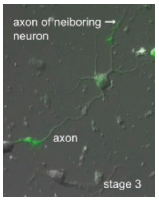

Video 1. **Accumulation of CA-KIF5C to the tips of a future axon in MAP2 (−/−) hippocampal neurons in stage 2-to-3 transition.** Hippocampal cells from MAP2 (−/−) embryos were cultured and transfected with K381-YFP cDNA by electroporation. Time-lapse images were obtained at 37°C at 10-min intervals, from 36 h after dissociation using an autofocus multiple-point inverted microscope (IX-72 ZDC; Olympus) equipped with a cooled CCD camera. Note, K381-YFP switches neurites at stage 2 and accumulates to axonal tips at stage 3 (arrows), similar to wild-type neurons.

References

Nakata, T., and N. Hirokawa. 2003. Microtubules provide directional cues for polarized axonal transport through interaction with kinesin motor head. *J. Cell Biol.* 162:1045–1055. doi:10.1083/jcb.200302175

van de Linde, S., U. Endesfelder, A. Mukherjee, M. Schüttpelz, G. Wiebusch, S. Wolter, M. Heilemann, and M. Sauer. 2009. Multicolor photoswitching microscopy for subdiffraction-resolution fluorescence imaging. *Photochem. Photobiol. Sci.* 8:465–469. doi:10.1039/b822533h